Journal of Integrative Agriculture 2018, 17(1): 94–110

Available online at www.sciencedirect.com

ScienceDirect

RESEARCH ARTICLE

Identification of salinity-related genes in *ENO2* mutant (*eno2*$^{-}$) of *Arabidopsis thaliana*

ZHANG Yong-hua[1], CHEN Chao[2], SHI Zi-han[1], CHENG Hui-mei[1], BING Jie[1], MA Xiao-feng[1], ZHENG Chao-xing[1], LI Hong-jie[3], ZHANG Gen-fa[1]

[1] *Beijing Key Laboratory of Gene Resource and Molecular Development/College of Life Sciences, Beijing Normal University, Beijing 100875, P.R.China*

[2] *Beijing Normal University, Zhuhai 519087, P.R.China*

[3] *National Key Facility for Crop Gene Resources and Genetic Improvement/Institute of Crop Sciences, Chinese Academy of Agricultural Sciences, Beijing 100081, P.R.China*

Abstract

Abiotic stress poses a great threat to plant growth and can lead to huge losses in yield. Gene *enolase2* (*ENO2*) is important in resistance to abiotic stress in various organisms. *ENO2* T-DNA insertion mutant (*eno2*$^{-}$) plants of *Arabidopsis thaliana* showed complete susceptibility to sodium chloride treatment when were analyzed either as whole plants or by measuring root growth during NaCl treatment. Quantitative real-time RT-PCR (RT-qPCR) was performed to investigate the expression profile of *ENO2* in response to NaCl stress in *Arabidopsis*. The transcript level of *ENO2* was rapidly elevated in 300 mmol L^{-1} NaCl treatment. ENO2 also responded to 300 mmol L^{-1} NaCl treatment at the protein level. To illuminate the mechanism underlying *ENO2* resistance to salt at the transcriptional level, we studied the wild-type and *eno2*$^{-}$ *Arabidopsis* lines that were treated with 300 mmol L^{-1} NaCl for 18 h using 454 GS FLX, which resulted in an expressed sequence tag (EST) dataset. A total of 961 up-regulated and 746 down-regulated differentially expressed genes (DEGs) were identified in the pairwise comparison WT-18 h:*eno2*$^{-}$-18 h. The DEGs were identified and functionally annotated using the databases of Gene Ontology (GO) and the Kyoto encyclopedia of genes and genomes (KEGG). The identified unigenes were subjected to GO analysis to determine biological, molecular, and cellular functions. The biological process was enriched in a total of 20 GO terms, the cellular component was enriched in 13 GO terms, and the molecular function was enriched in 11 GO terms. Using KEGG mapping, DEGs with pathway annotations contributed to 115 pathways. The top 3 pathways based on a statistical analysis were biosynthesis of the secondary metabolites (KO01110), plant-pathogen interactions (KO04626), and plant hormone signal transduction (KO04075). Based on these results, *ENO2* contributes to increased resistance to abiotic stress. In particular, *ENO2* is involved in some of the metabolic stress response pathways in *Arabidopsis*. Our work also demonstrates that this EST dataset will be a powerful resource for further studies of *ENO2*, such as functional analyses, investigations of biological roles, and molecular breeding. Additionally, 3-phosphoglycerate kinase (PGK), 3-phosphoglycerate

Received 6 December, 2016 Accepted 5 May, 2017
Correspondence ZHANG Gen-fa, Tel: +86-10-58809453, E-mail: gfzh@bnu.edu.cn; LI Hong-jie, Tel: +86-10-82105321, E-mail: lihongjie@caas.cn

doi: 10.1016/S2095-3119(17)61720-9

kinase 1 (PGK1), triosephosphate isomerase (TPI), and pyruvate kinase (PK) in glycolysis interactions with ENO2 were verified using the yeast two-hybrid experiment, and *ENO2* may regulate the expression of *PGK*, *PGK1*, *TPI*, and *PK*. Taken together, the results from this study reflects that *ENO2* gene has an important role in the response to the high salt stress.

Keywords: *ENO2*, NaCl tolerance, abiotic stress, 454 GS FLX sequencing, GO, KEGG

1. Introduction

In nature, plants are exposed to complex environmental conditions with different abiotic stresses such as drought, high temperature, chilling injury, metal toxicity, salinity, hypoxia, and water logging, which influence plant growth and development (Bray *et al*. 2000; Bent and Mackey 2007; Ahmad and Prasad 2012; Shi *et al*. 2013; Parimalan *et al*. 2014). Abiotic stresses were estimated to cause decline of up to 50–70% in major crop productivities (Mittler 2006). Therefore, abiotic stresses are serious problem in agriculture worldwide. In the past decades, studies on the molecular basis of the plant response to these abiotic stresses have been a major focus of research. A number of genes/pathways and regulatory networks were responsive to the tolerance to abiotic stresses in plants (Mickelbart *et al*. 2015). Numerous studies have indicated that NAC transcription factors (TFs), *AP2/EREBP*, *MYB*, *WRKY* or *bZIP* families, and some *TF* genes are effective in the improvement of stress resistance in model plant species and crops of economic importance (Shao *et al*. 2015; Wang *et al*. 2016). The effects of hormones in abiotic stress responses have been examined (Pieterse *et al*. 2012; Liu *et al*. 2013).

Enolase (ENO) is highly expressed in certain organisms during glycolysis, a vital metabolic pathway (Holland *et al*. 1978). It functions in the transformation of 2-phosphoglycerate to phosphoenolpyruvate (Reed *et al*. 1996). Some *ENO* genes encoding this enzyme have been cloned from various plant species, including *Mesembryanthemum crystallinum* L., *Arabidopsis* (van der Straeten *et al*. 1991), *Castor bean* Latin (Blakeley *et al*. 1994), *Oryza sativa* L. (Umeda *et al*. 1994), *Lycopersicon esculentum* Mill (van der Straeten *et al*. 1991), *Zea mays* L. (Lal *et al*. 1991), and *Nicotiana tabacum* L (Voll *et al*. 2009). In *Arabidopsis*, *ENO2* is the highly expressed *enolase* (Andriotis *et al*. 2010). As a bifunctional locus, it encodes AtENO2 and AtMBP-1 (*A. thaliana* cMyc-binding protein) as a positive regulator in response to ABA treatment (Kang *et al*. 2013). To date, AtMBP-1 has been identified as an ENO2 transcription repressor that mediates glycolysis (Eremina *et al*. 2015). *ENO2* is also required for abiotic stress responses (Sachs *et al*. 1980; Lee *et al*. 2002; Ndimba *et al*. 2005; Yan *et al*. 2005; Jiang *et al*. 2007; Barkla *et al*. 2009). Therefore, research investigating the *ENO2* gene is important owing to its involvement in vital glycolysis and stress tolerance pathways as functional gene or transcription factor in plants.

We generated the *ENO2* T-DNA insertion mutant (*eno2*$^{-}$). Compared to the wild type (WT), this mutant displayed some phenotypic changes, such as reduced shoot and root growth, impaired male gametophyte organogenesis, and shortened siliques, as well as a reduced number of seeds. Our results were different from that of Eremina *et al*. (2015) who found that the development of female and male organs and the male gametophyte function required ENO2, and the fertility is reduced as a consequence of defects in ENO2. Bray (1997) suggested that the genotype, species, and phenotypic traits all affected the responses to abiotic stresses. Barkla *et al*. (2009) showed that a single point mutation (G325S) allele exhibited a reduction in ENO protein specifically in tonoplast that was induced by salinity. In this study, we found that *eno2*$^{-}$ plants were completely susceptible to NaCl stress. Thus, we studied the expression profiles of *AtENO2* during NaCl stress treatment using RT-qPCR and Western blotting. The results demonstrated that the transcript levels of *AtENO2* were rapidly increased in response to treatment with 300 mmol L^{-1} NaCl. ENO2 also responds to 300 mmol L^{-1} NaCl stress at the protein level. To further unravel the mechanism of *AtENO2* in responses to abiotic stress in plants, we adopted the 454 GS FLX sequencing method because it facilitates the identification and quantification of numerous transcripts (Rothberg *et al*. 2008). Global analysis of high-throughput sequencing in species exposed to different stress conditions will facilitate the identification of specific pathways and genes responsible for tolerance to a particular stress (Rangan *et al*. 2014). To generate a global perspective of the salinity-induced alterations at the transcriptomic level and the salinity-responsive metabolic pathways in the WT and *eno2*$^{-}$ mutant *Arabidopsis*, 454 GS FLX sequencing was performed with the leaves collected from the salinity-stressed WT and *eno2*$^{-}$ plants using the Ion Proton platform. We identified many differentially expressed genes (DEGs), which were functionally annotated using the GO and KEGG databases. The analyzed DEGs were associated with plant-pathogen interactions, plant hormone signal transduction, and the glycolysis pathway in KEGG. Beyond that, we determined whether ENO2 interacts with PGK, PGK1, TPI, PK, and GAPC1, which are also the key

enzymes of glycolytic pathway. Based on these findings, we explored the effect of *ENO2* on its interaction protein genes by RT-qPCR. This study improves our understanding of *ENO2* and supports its importance in the survival of plants exposed to abiotic stress.

2. Materials and methods

2.1. Plant materials and stress treatment

The *eno2*$^-$ mutant plants were obtained progressively from T_0 through T_3 by the addition of 50 μg mL^{-1} of kanamycin (Kan) to the Murashige and Skoog (MS) medium. After surface-sterilizing with 0.1% (w/v) $HgCl_2$ solution, seeds were allowed vernalization in the dark for at least 3 d at 4°C. Then, they were sown on MS plates (pH 5.8) containing 3% sucrose as the source of carbon and 0.7% (w/v) agar for solidification. The plants were grown at 22°C with a photoperiod of 16-h light/8-h dark and a relative humidity of 70%.

To measure root growth, seedlings were grown on MS plates supplemented with appropriate concentrations of NaCl. After 10 d, root length of seedlings was measured. For evaluation of salinity resistance, 30-d-old plants were further grown in a mixture of soil and vermiculite (3:1) for treatment with 300 mmol L^{-1} NaCl.

To study the expression profile of *ENO2* (GenBank accession no. NM_129209.3) under the salt-stress, wild-type *Arabidopsis* seedlings at the 4–6 leaf stage were transferred to the plastic pots containing a mixture of vermiculite and perlite (3:1, v/v) and watered with the Hoagland nutrient solution supplemented with 100, 150, 200, or 300 mmol L^{-1} NaCl for 0, 2, 4, 6, 8, 10, 12, 24, 36, or 48 h. To study the expression levels of *ENO1*, *ENO2* and *ENO3* under the salt stress, 30-d-old WT and *eno2*$^-$ plants were treated with 300 mmol L^{-1} NaCl for 0, 18, or 24 h. To survey the expression profile of *ENO2* or ENO2 in the presence of cold, heat, drought, and salt stresses, 30-d-old WT plants were treated with 4°C, 28°C, 20% PEG 600, or 300 mmol L^{-1} NaCl.

2.2. RNA extraction

Total RNA was purified from the leaves grown under the control or different salt stress conditions using the One-Step RNA Reagent (TransGen, Beijing, China). The RNA from each sample (2.5 μg) was used for reverse transcription with a cDNA Synthesis Kit (TransGen, Beijing, China) and then used in quantitative real-time RT-PCR (RT-qPCR) analysis. More than 10 μg of RNA per sample were purified using an RNeasy Plant Mini Kit (Qiagen, Valencia, CA, Spain). Total RNA was quantified using a Bioanalyzer 2100 (Agilent Technologies, Santa Clara, CA, USA) and a NanoDrop spectrophotometer (Thermo Fisher Scientific, Wilmington, DE, USA). These RNA are designed for 454 GS FLX sequencing.

2.3. Quantitative real-time RT-PCR analysis

Quantitative real-time RT-PCR was performed on an ABI 7500 System (Applied Biosystems, Foster City, CA, USA) with the SYBR green detection using a *TransStart*® Green qPCR SuperMix Kit (TransGen, Beijing, China). The *ENO2* gene was analyzed in triplicate and at least three biological replicates. The average threshold cycle (C_t) was then calculated for each sample. The $2^{-\Delta\Delta Ct}$ method was used to calculate the relative expression levels. The expression of *β-actin* was measured in parallel as an endogenous control. For examining the expression profile of *ENO2* under salt stress conditions, the control sample served as the calibrator with a nominal value of 1. The primers used in RT-qPCR for *ENO1*, *ENO2*, *ENO3*, *CNGCs*, *AUX1*, *AHP*, *ATFBA7*, and *β-actin* are shown in Appendix A.

2.4. Protein extraction

Proteins from the WT and *eno2*$^-$ mutant leaves were extracted in 50 mmol L^{-1} Tris-HCl, 150 mmol L^{-1} NaCl, 10% glycerol, 0.1% Nonidet P-40, 5 mmol L^{-1} dithiothreitol (DTT), and 0.1% Triton X-100 with vigorous vortexing. After incubation on ice for 30 min, the supernatant was produced by centrifugation at 13 000×g and 4°C for 15 min. The protein concentration was determined using the bicinchoninic acid (BCA) assay (Dingguo Changsheng, Beijing, China).

2.5. Western blotting analysis

The protein samples (20 μg each) were separated on 12% sodium dodecyl sulfate-polyacrylamide gel electrophoresis (SDS-PAGE) prior to transferring to nitrocellulose membranes (Pall, New York, NY, USA). Rabbit polyclonal antibody was prepared by BGI-Tech Solutions Co., Ltd. (BGI-Tech, Shenzhen, China). The membrane was blocked by Tris-buffered saline (TBS) containing 5% milk for 1 h at room temperature. The primary antibody (rabbit poly-clonal ENO2 and mouse β-actin antibodies) was prepared in the TBS buffer (1:3 000). After washing in the TBST buffer (TBS containing 0.05% Tween-20) to remove unbound antibodies, the blot was incubated with the goat anti-rabbit IgG conjugated to horseradish peroxidase and sheep anti-mouse secondary antibodies in TBST buffer at a dilution of 1:3 000, and the results were visualized using enhanced chemiluminescent reagents (Pierce, Appleton,

WI, USA).

2.6. Library preparation and sequencing

Total RNA from the WT and *eno2*$^{-}$ plants treated with 300 mmol L^{-1} NaCl for 18 h was converted to cDNA. After removing the rRNA, the samples were sequenced using the 454 GS FLX platform. Briefly, mRNA was purified from 8 μg of total RNA, a mixture of RNA from WT or *eno2*$^{-}$ leaves exposed to high salinity of 300 mmol L^{-1} for 18 h, using oligo(dT) magnetic beads. The cDNA fragments produced by divalent cations under elevated temperature were subjected to an end repair process and adapter ligation. These products were purified and enriched to create the final cDNA library. Additionally, Ion Proton sequencing was performed by BGI Tech Solutions Co., Ltd. (Shenzhen, China).

2.7. Differential gene expression analysis

In the 454 GS FLX study, we used the reads per kb per million reads (RPKM) method to analyze the gene expression profiles. Using a 0.1% or less false discovery rate (FDR), genes that exhibited a change of two-fold or greater were regarded as differentially expressed genes (DEGs). A DEG was considered up-regulated if its expression level in the *eno2*$^{-}$ sample was significantly higher than those in the WT sample, while a down-regulated DEG was identified if the expression level in the WT was greater than that in the *eno2*$^{-}$ sample.

2.8. Analyses of Gene Ontology (GO) and pathway

The assembled sequences were compared against the public non-redundant protein sequences (Nr) database. According to the obtained Nr annotation, all DEG annotation information was collected in the Blast2GO software (Conesa *et al*. 2005). GO terms are assigned to query sequences, resulting in a group of genes that were cataloged in the transcriptome for separate ontology vocabularies, biological processes, molecular functions, and cellular components (Altschul 1993). Furthermore, pathway-based analysis improves our understanding of the biological functions of genes, and all DEGs were mapped to terms in the Kyoto encyclopedia of genes and genomes (KEGG) database.

2.9. Yeast two-hybrid assays

To assess protein interactions, yeast two-hybrid assay was carried out following the instructions of BD Matchmaker Library Construction & Screening Kits (Clontech, PaloAlto, CA, USA). The full-length cDNAs of *PGK*, *PGK1*, *TPI*, *PK*, *GAPC1*, and *ENO2* were amplified separately. The primers used are shown in Appendix A. The cDNAs of *PGK*, *PGK1*, *TPI*, *PK*, and *GAPC1* were cloned into pGADT7 to be used as the prey vector pGADT7-PGK, pGADT7-PGK1, pGADT7-TPI, pGADT7-PK, and pGADT7-GAPC1. The cDNA of *ENO2* was cloned into pGBKT7 to be used as the bait vector pGBKT7-ENO2. The resulting pGADT7-PGK, pGADT7-PGK1, pGADT7-TPI, pGADT7-PK, pGADT7-GAPC1, and each bait vector were co-transformed into yeast strain AH109. The resulting bait vector and empty prey vector were also co-transformed into yeast strain AH109. The transformed colonies were identified on yeast SD/-Trp-Leu (DDO) and SD/-Trp-Leu-His-Ade (QDO) medium.

2.10. Statistical analysis

All the experiments were repeated at least three times, and all the data are presented as means±standard deviations (SD). One-way analysis of variance (ANOVA) was performed for all the data and the significance of difference in values (P<0.05 or P<0.01) was determined by the Fisher's least significant difference (LSD) test using SPSS 20.0 for Windows.

3. Results

3.1. The WT exhibited superior salinity tolerance compared to *eno2*$^{-}$

Salt stress had an obvious effect on the root growth at the 10th day after germination in the WT and *eno2*$^{-}$ plants. The root growth was significantly different between the WT and *eno2*$^{-}$, even though they were grown under normal conditions. Compared to the WT, the root length of *eno2*$^{-}$ plant had reduced by half under regular growth condition (Fig. 1-A), with the *eno2*$^{-}$ plants exhibiting a shorter root length. Root elongation of the WT and *eno2*$^{-}$ was significantly reduced even by 50 mmol L^{-1} NaCl, and the *eno2*$^{-}$ root length was only 1/4 of WT root length, which indicates increased sensitivity to NaCl stress (Fig. 1-A). Root elongation decreased in the WT and *eno2*$^{-}$ on MS medium supplemented with 100 mmol L^{-1} NaCl. In particularly, the *eno2*$^{-}$ root growth was greatly inhibited, suggesting the *eno2*$^{-}$ was much more sensitive to salt than the WT (Fig. 1-A). Thus, the root growth of *eno2*$^{-}$ plants was greatly inhibited under the same conditions. The *eno2*$^{-}$ mutant was sensitive to salt stress based on root growth. This result indicates that *ENO2* is involved in the response of *Arabidopsis* to salt stress. Thus, the comparison of the tolerance to NaCl between the *eno2*$^{-}$ mutant and the WT was conducted by treatment of 30-d-old plants grown under normal conditions with 300 mmol L^{-1} NaCl for 21 d.

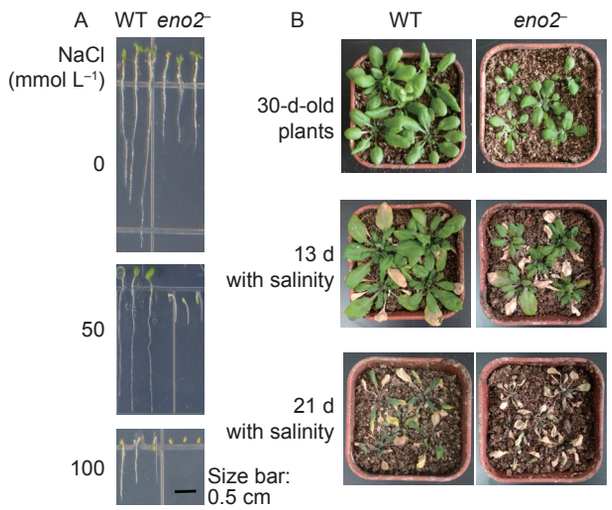

Fig. 1 Estimation of the salt stress tolerance of the wild-type (WT) and *ENO2* T-DNA insertion mutant (*eno2*$^{-}$) plants. A, root growth of the WT and *eno2*$^{-}$ plants in response to 0, 50, or 100 mmol L^{-1} NaCl for 10 d. B, salt tolerance of the WT and *eno2*$^{-}$ plants. 7-d-old seedlings were transferred to soil for an additional 23 d of normal growth (upper panel) and subjected to progressive salinity by the application of 300 mmol L^{-1} NaCl for 13 d (middle panel) and for 21 d (lower panel).

During the period of salt stress, most WT plants and almost all the *eno2*$^{-}$ plants displayed severe withering (Fig. 1-B). At least 40 strains of the WT and *eno2*$^{-}$ plants were treated separately with NaCl. We randomly chose a plate from the reproducible results (Fig. 1-B). This suggests that the loss-of-function of *ENO2* compromised salt tolerance. Thus, *ENO2* promotes salt tolerance in plants.

3.2. Salinity-responsive transcription and protein changes in the WT plants

To determine whether *ENO2* expression is induced by salt stress, RT-qPCR analysis was carried out using total mRNA that were purified from the 30-d-old plants grown either under 100, 150, 200, or 300 mmol L^{-1} NaCl treatment or normal condition. The mRNA levels in *ENO2* increased in the plants exposed to 300 mmol L^{-1} NaCl by approximately 11-fold at 18 h. The expression of *ENO2* at 6 h exposure at 150 mmol L^{-1} NaCl took the second place. *ENO2* mRNA showed lower induction from 0.3- to 10-fold by the treatment of other salt conditions. However, The ENO2 mRNA levels were reduced to a low level approximately equaling the control at 24 h (Fig. 2-A). *Arabidopsis* contains three *ENOs*: *ENO1*, *ENO2*, and *ENO3/ENOc*. Consequently, we also studied *ENO1* and *ENO3* for the comparison to *ENO2* between the WT and *eno2*$^{-}$ plants. The *ENO2* transcript level was the highest, followed by *ENO1* and *ENO3* (Fig. 2-B). Among the three *ENO* genes, *ENO2* was clearly the most important in response to salt stress. To confirm whether the expression of *ENO2* was induced by other abiotic stresses in addition to salt, we performed RT-qPCR analysis to detect the expression pattern of *ENO2*. The transcript level of *ENO2* increased dramatically upon exposure to salt. Salt was a more effective trigger for the transcription of *ENO2* in comparison to cold, heat, and drought (Fig. 2-B). This indicates that *ENO2* functions in the rapid response to salt stress in *Arabidopsis*. With an extended response time, it is possible that other defense genes or pathways play vital roles in resistance to salt damage. Moreover, we evaluated changes in ENO2 protein expression in the WT plants suffering from cold, heat, drought, or salt stress by Western blotting. Clear differences were observed in the abundance of ENO2 protein in response to these abiotic stresses. Analysis of the control and the cold, heat, drought, or salt-stressed samples revealed that ENO2 protein was significantly altered in response to short-term salt stress. Likewise, cold, heat, or drought stress also enhanced the levels of ENO2, albeit to a lesser degree than salt stress. However, ENO2 accumulation was not obviously affected by drought stress at 24 h (Fig. 2-D). These results demonstrated that *ENO2* is involved in the response to salt stress in *Arabidopsis*.

3.3. Sequence assembly and mapping statistics

It should be noted that, after pre-processing, reads shorter than 30 bp were excluded; after trimming the adapter sequence, each of sequences that were less than the length of the set threshold was also excluded (Fig. 3). The raw data were then converted to clean data, which were used for subsequent analyses.

Table 1 shows an overview of the genome sequencing and mapping results. RNA sequencing on a 454 GS-FLX provided 2.71 and 2.77 billion base pairs from the WT and *eno2*$^{-}$ plants, respectively. In each dataset, 18.88 and 19.25 million sequences matched perfectly with known genes. A total of 17 260 006 (63.76%) and 17 754 183 (64.08%) unique matches in each dataset were also obtained. The annotated reference assembly was downloaded for the reference genes (ftp://ftp.arabidopsis.org/home/tair/Genes/TAIR10_genome_release/TAIR10_blastsets/TAIR10_cdna_20101214_updated).

For the WT, out of 27 071 011 total reads, 27 004 513 (99.75%) were mapped to unique positions in the genome, and 26 530 577 (98.00%) reads showed unique matches to the genome. For *eno2*$^{-}$, of 27 707 416 total reads, 27 636 225 (99.74%) reads were mapped to unique positions in the genome, and 27 242 599 (98.32%) reads showed unique matches to the genome. The annotated reference was downloaded from TAIR10.

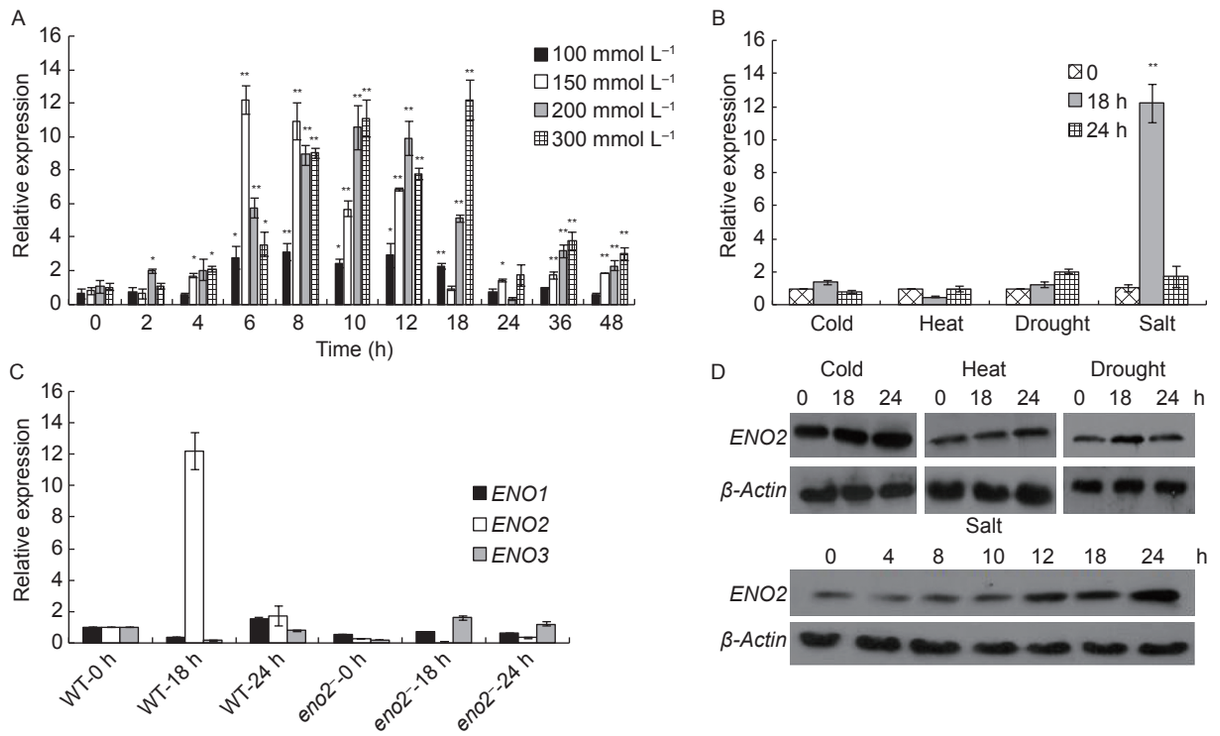

Fig. 2 Expression of *enolase* (*ENO*) in response to different abiotic stresses in the wild-type (WT) and *ENO2* T-DNA insertion mutant (*eno2*$^{-}$) plants. A, expression of *ENO2* under salt stress as determined by quantitative real-time RT-PCR (RT-qPCR) analysis. B, the expression of *ENO1*, *ENO2*, and *ENO3* under the salt stress as determined by RT-qPCR analysis. C, the expression of *ENO2* in the presence of cold, heat, drought, and salt stresses, as revealed by RT-qPCR analysis. A–C, data are the means±standard deviation (SD) of three replicates. D, the expression of *ENO2* in response to cold, heat, drought and salt stresses, as revealed by Western blot analysis. * and **, significances at $P<0.05$ and $P<0.01$, respectively.

All unigenes were further classified with specific annotations using standardized Gene Ontology (GO) vocabulary. The available biological information was analyzed at $P\leq0.01$ by pairwise comparisons, i.e., WT-18 h: *eno2*-18 h.

3.4. Functional annotation (GO analysis)

Biological process was enriched in a total of 20 GO terms, cellular component in 13 GO terms, and molecular function in 11 GO terms (Fig. 4).

GO: Biological process Biological process enrichment was observed for 3 668 genes in 20 GO terms, ranging from 4 to 742 genes. Most identified unigenes were predicted in the metabolic process (742 genes), cellular process (697 genes), response to stimulus (568 genes), and single-organism process (372 genes). In addition, there were identified unigenes predicted in the response to stress (67 genes), response to osmotic stress (40 genes), response to metal ion (27 genes), response to abiotic stimulus (21 genes), cellular response to stress (12 genes), response to biotic stimulus (12 genes), response to salt stress (2 genes), and cellular response to stimulus (2 genes). This finding suggests that the defense system and metabolic pathways are activated.

GO: Cellular component Cellular component enrichment was observed for 3 254 genes ranging from 2 to 905 genes in 13 GO terms. Most identified unigenes were associated with cell (905 genes), cell part (905 genes), organelle (575 genes), and membrane (354 genes).

GO: Molecular function Molecular function enrichment was observed for 1 689 genes with a range of 1 to 720 genes in 11 GO terms. Most of the unigenes were involved in binding (720 genes), followed by catalytic activity (657 genes).

3.5. Differential gene expression between *eno2*$^{-}$ and the WT

Differential gene expression during the progression of stress reveals stress responsiveness and its putative role in stress tolerance. The DEGs are genes with a $\log_2$(fold change) ratio≥1 and false discovery rate (FDR)≤0.001 based on the DESeq software (Fig. 5). A total of 961 sequences were categorized as up-regulated genes and 746 sequences were categorized as down-regulated genes

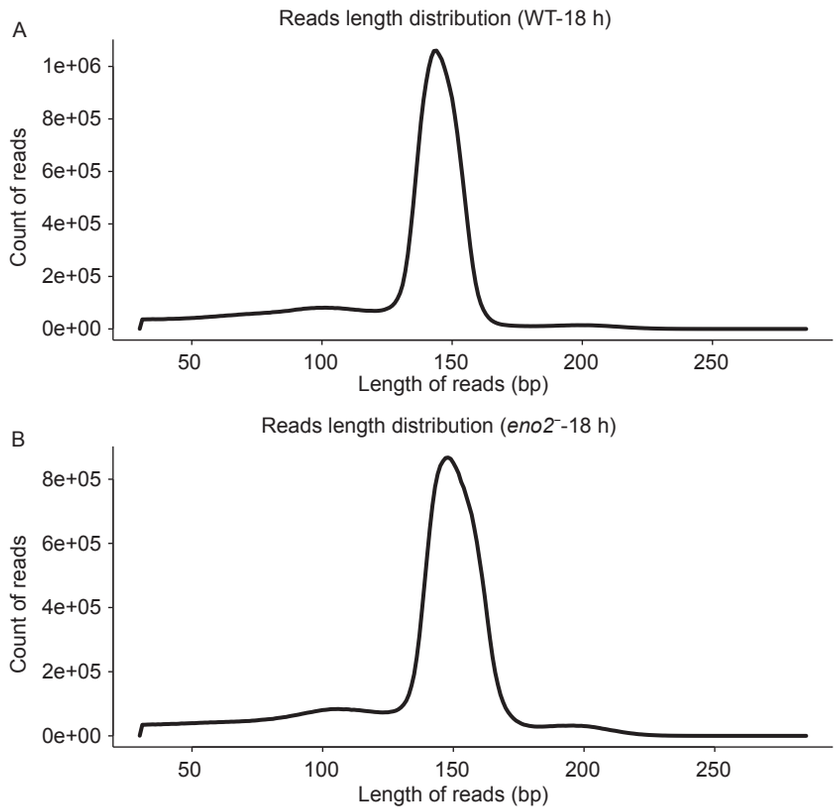

Fig. 3 Sequence length distribution of the wild-type (WT) and *ENO2* T-DNA insertion mutant (*eno2*$^{-}$) libraries. A, size distribution of 454 sequencing reads after trimming of adapter and short reads (<30 bases) for the *Arabidopsis* WT. B, size distribution of 454 sequencing reads after trimming of adapter and short reads (<30 bases) for *Arabidopsis eno2*$^{-}$.

in *eno2*$^{-}$ compared to the WT. The detected fold changes ($\log_2$ratio) in gene expression ranged from –10.6 to 12.8. The most up-regulated known gene was *AT1G67265.1*, which encodes ROTUNDIFOLIA like 21, followed by AT1G29510.1, encoding a SAUR-like auxin-responsive protein family. The most down-regulated known genes |$\log_2$ratio (*eno2*$^{-}$-18 h/WT-18 h)≥10| were AT5G11140.1, which encodes *Arabidopsis* phospholipase-like protein (PEARLI 4); AT3G21520.1, encoding a DUF679 domain membrane protein 1 (AtDMP1); AT1G42050.1 and AT1G42040.1, encoding transposable element genes; AT2G26400.1, encoding acireductone dioxygenase 3 (ARD3); AT1G33760.1, encoding an integrase-type DNA-binding superfamily protein; AT2G23830.1, encoding a papD-like superfamily protein; and AT5G02780.1, encoding glutathione transferase lambda 1 (GSTL1). In addition, many well-characterized salt response genes were found among these DEGs. For example, AT3G09260.1 encoding the β-glucosidase 23, AT2G24850.1 encoding the tyrosine aminotransferase 3, and AT1G19210.1 encoding the ethylene-responsive transcription factor ERF017 were up-regulated. AT3G48360.1 encoding the BTB and TAZ domain protein 2 and AT1G71030.1 encoding the v-myb avian myeloblastosis viral oncogene homolog (MYB)-related transcription factor were down-regulated.

3.6. *eno2*$^{-}$-specific gene expression profile

In an attempt to determine the *eno2*$^{-}$-associated expression of DEGs, the expression of 7 genes was assessed. Among them, DEGs, such as AT1G09930.1 (oligopeptide transporter 2), AT1G21850.1 (SKU5 similar 8 protein), AT1G68765.1 (protein IDA), AT2G39530.1 (UPF0497 membrane protein), AT4G11170.1 (similar to several *A. thaliana* disease resistance proteins), AT5G11140.1 (phospholipase-like (PEARLI 4) family protein), and AT5G24110.1 (WRKY DNA-binding protein 30), were detected. Results of GO analysis indicated that 6 of these genes were enriched in the categories of response to abiotic stimulus, metabolic process, light stimulus, response to hormone stimulus, defense response, response to osmotic stress, response to stress, and transcription DNA-dependent. The KEGG analysis revealed that AT1G21850.1, AT4G11170.1, and AT5G24110.1, which function as an L-ascorbate oxidase [EC:1.10.3.3], the disease resistance protein RPS2, and the WRKY transcription factor 29, were separately enriched in

Table 1 Number and percentage of reads mapped to reference gene and genome[1)]

	WT-18 h (mapping to gene)		WT-18 h (mapping to genome)		*eno2*$^{-}$-18 h (mapping to gene)		*eno2*$^{-}$-18 h (mapping to genome)	
	Reads number	Percentage (%)	Reads number	Percentage (%)	Reads number	Percentage (%)	Reads number	Percentage (%)
Total reads	27 071 011	100	27 071 011	100	27 707 416	100	27 707 416	100
Total base pairs	3.61E+09	100	3.61E+09	100	3.86E+09	100	3.86E+09	100
Total mapped reads	26 887 025	99.32	27 004 513	99.75	27 514 289	99.30	27 636 225	99.74
Perfect match	18 880 188	69.74	17 584 242	64.96	19 253 500	69.49	17 875 314	64.51
Mismatch	8 006 837	29.58	9 420 271	34.80	8 260 789	29.81	9 760 911	35.23
Unique match	17 260 006	63.76	26 530 577	98.00	17 754 183	64.08	27 242 599	98.32
Multi-position match	9 627 019	35.56	473 936	1.75	9 760 106	35.23	393 626	1.42
Total unmapped reads	183 985	0.68	66 497	0.25	193 126	0.70	71 190	0.26

[1)]WT, wild type; *eno2*$^{-}$, *ENO2* T-DNA insertion mutant.

PATH: map00423, PATH: map13457, and PATH: map13424, respectively.

3.7. KEGG analysis

To identify the biological pathways that were altered by *ENO2* in response to salt stress, up- and down-regulated DEGs were assigned to KEGG pathways with enrichment statistics (Fig. 6). In the KEGG mapping, the DEGs with pathway annotations contributed to 115 pathways. The top 3 pathways (sorted by the *q*-value) were biosynthesis of the secondary metabolites (PATH: map01110), plant-pathogen interaction (PATH: map04626), and plant hormone signal transduction (PATH: map04075). The pathways with the largest number of genes were sorted as follows: biosynthesis of the secondary metabolites with 159 (16.56%) DEGs, plant-pathogen interaction with 131 (13.65%) DEGs, and plant hormone signal transduction with 90 (9.38%) DEGs. However, there was no map of biosynthesis of the secondary metabolites in the KEGG database for DEGs identified. Consequently, we focused on map04626 and map04075 because both of them are important stress adaptation pathways.

Numerous salinity-responsive DEGs in the contrasting WT-18 h and *eno2*$^{-}$-18 h were mapped onto the plant-pathogen interaction pathways using the KEGG database. The mapping revealed that the genes involved in the plant-pathogen interaction processes were significantly affected during salinity stress, followed by kinase, transcription factors, defensive protein and genes involved in signal transduction (Fig. 7). The following 15 up-regulated protein families were identified, including cyclic nucleotide gated channel (CNGCs), calcium-dependent protein kinase (CDPK, EC:2.7.11.1), calmodulin/calcium-binding protein (CMLCaM/CML), mitogen-activated protein kinase kinase 1 (MEKK1, EC:2.7.11.25), WRKY transcription factor 25/29/33 (WRKY25/29/33), pathogenesis-related protein 1 (PR1), RPM1-interacting protein 4 (RIN4), disease resistance protein RPM1 (RPM1), disease resistance protein RPS2 (RPS2), heat shock protein 90 kDa beta (HSP90), jasmonate ZIM domain-containing protein (JAZ), and transcription factor MYC2 (MYC2). Only 2 protein families were down-regulated: respiratory burst oxidase (Rboh, EC:1.6.3.-1.11.1.-) and somatic embryogenesis receptor kinase (BKK1, EC:2.7.10.1 2.7.11.1). Interestingly, 5 protein families were up- and down-regulated simultaneously: chitin elicitor receptor kinase 1 (CERK1), LRR receptor-like serine/threonine-protein kinase FLS2 (FLS2, EC:2.7.11.1), brassinosteroid insensitive 1-associated receptor kinase 1 (BAK1, EC:2.7.10.1 2.7.11.1), WRKY transcription factor 22 (WRKY22), and serine/threonine-protein kinase PBS1 (PBS1, EC:2.7.11.1).

Mapping of the DEGs onto plant hormone signal transduction pathways using the KEGG database revealed a clear effect on the following hormones during salinity stress: auxin, cytokinin, gibberellin, abscisic acid, ethylene, brassinosteroid, jasmonic acid, and salicylic acid (Fig. 8). During auxin biosynthesis, most protein or protein families were changed. Three proteins, auxin influx carrier (AUX1 LAX family), transport inhibitor response 1 (TIR1), and auxin responsive *GH3* gene family (GH3) were up-regulated. Auxin response factor (ARF) was down-regulated. Auxin-responsive protein IAA (IAA) and SAUR family protein (SAUR) were up- and down-regulated simultaneously. In cytokinin biosynthesis, histidine-containing phosphotransfer protein (AHP), the two-component response regulator ARR-B family (ARR-B), and the two-component response regulator ARR-A family (ARR-A) were down-regulated. Histidine kinase 2/3/4 (cytokinin receptor, AHK2_3_4, EC:2.7.13.3) was up- and down-regulated. In the gibberellin biosynthesis, only the gibberellin receptor GID1 (GID1) was up-regulated. In abscisic acid biosynthesis, the abscisic acid receptor PYR/PYL family (PYL) was down-regulated. Protein

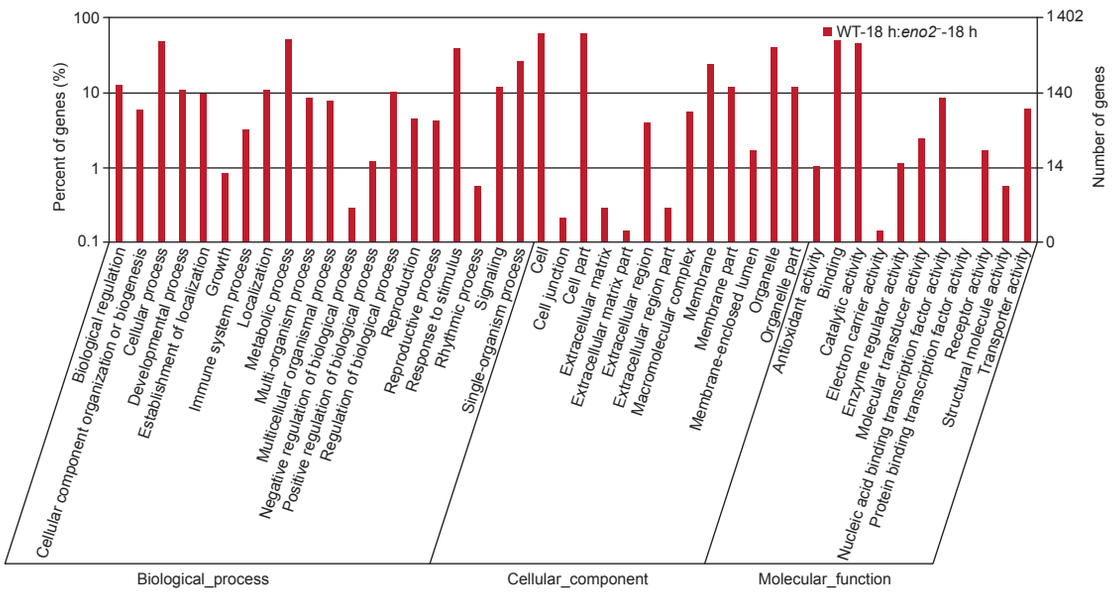

Fig. 4 Distribution of identified unigenes from wild-type (WT)-18 h:*ENO2* T-DNA insertion mutant (*eno2*$^{-}$)-18 h in the Gene Ontology (GO) term biological process, cellular component, and molecular function identified using the GO database (http://www.geneontology.org/).

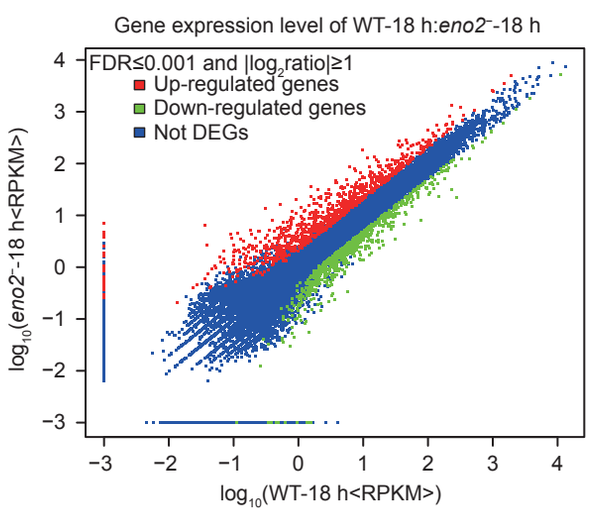

Fig. 5 Analysis of differentially expressed genes (DEGs) in the wild-type (WT)-18 h and *ENO2* T-DNA insertion mutant (*eno2*$^{-}$)-18 h mutant libraries. The red and green dots denote significantly different expression levels in each dataset (2-fold change), whereas the blue dot indicates no significant difference in gene expression. RPKM, reads per kilobase per million mapped reads.

phosphatase 2C (PP2C, EC:3.1.3.16), serine/threonine-protein kinase SRK2 (SNRK2, EC:2.7.11.1), and ABA responsive element binding factor (ABF) were up- and down-regulated. In ethylene biosynthesis, serine/threonine-protein kinase CTR1 (CTR1, EC:2.7.11.1) was down-regulated, but ethylene-responsive transcription factor 1 (ERF1) was up-regulated. In brassinosteroid biosynthesis, brassinosteroid insensitive 1-associated receptor kinase 1 (BAK1, EC:2.7.10.1 2.7.11.1) and protein brassinosteroid insensitive 1 (BRI1, EC:2.7.10.1 2.7.11.1) were up- and down-regulated. Brassinosteroid resistant 1/2 (BZR1_2) was down-regulated, and xyloglucan:xyloglucosyl transferase TCH4 (TCH4, EC:2.4.1.207) was up-regulated. In jasmonic acid biosynthesis, jasmonate ZIM domain-containing protein (JAZ) and the transcription factor MYC2 (MYC2) were up-regulated. In salicylic acid biosynthesis, the transcription factor TGA (TGA) was up- and down-regulated, and pathogenesis-related protein 1 (PR1) was up-regulated.

Because ENO2 catalyzes a key step in glycolysis, we examined glycolysis/gluconeogenesis (PATH: map00010) in 4 (0.42%) DEGs: AT2G36530.1 (*ENO2*), AT1G47860.1 (*LINE*), AT4G26520.1 (*ATFBA7*), and AT4G26270.1 (*PFK3*) (Fig. 9). The most down-regulated gene was AT2G36530.1 (*ENO2* gene). This result showed that *ENO2* was basically not expressed. Moreover, TFs (transcription factors) that are responsible for the expression of multiple downstream target genes (*LINE* and *ATFBA7*) in front of stress conditions were down-regulated. This result may be associated with the reduced salinity tolerance. Additionally, remedial key genes are critical during salt stress. The up-regulation of *PFK3* could influence the phosphorylation events controlling the stress signaling process. Such genetic modifications will lead to the activation of numerous down-stream response genes and provide salinity tolerance in plants.

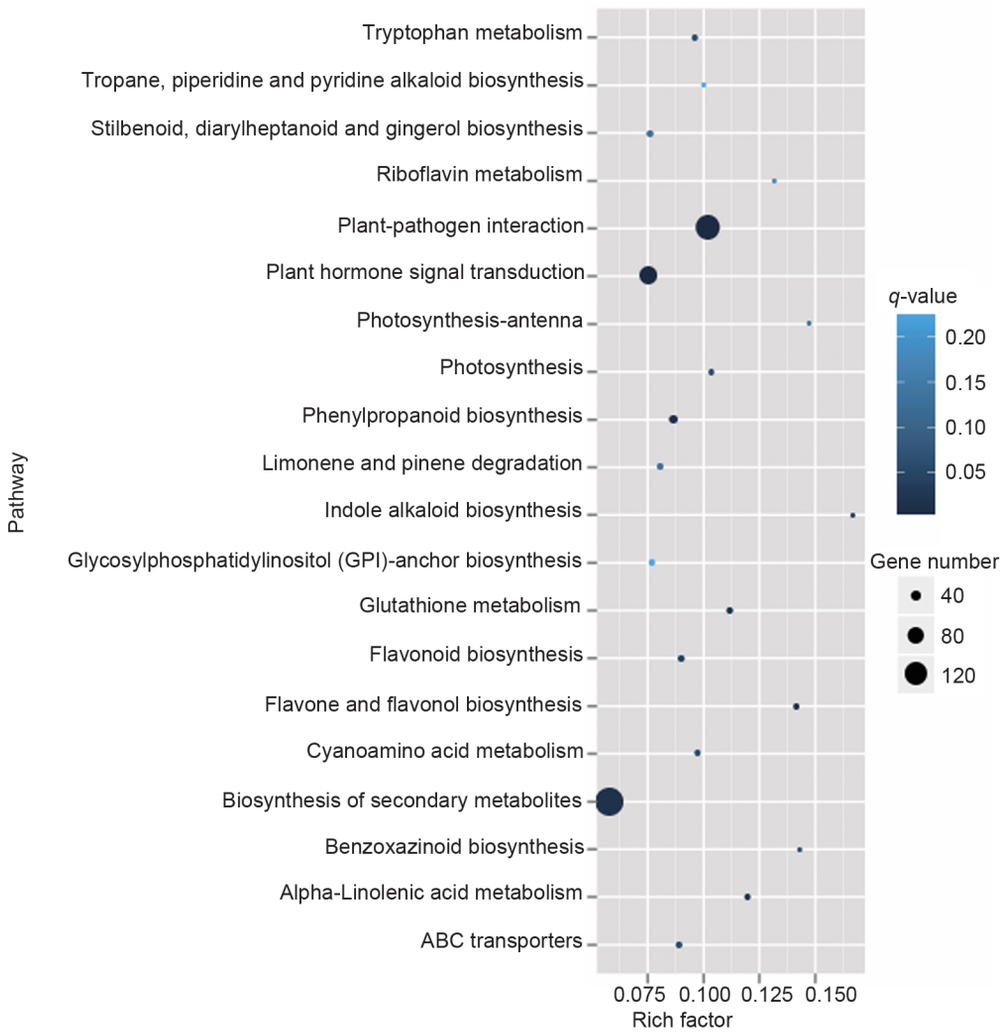

Fig. 6 Scatter plot of Kyoto encyclopedia of genes and genomes (KEGG) pathway enrichment statistics. The rich factor is the ratio of differentially expressed genes (DEGs) parsed in a given pathway to the total number of genes parsed in the same pathway. A greater rich factor indicates greater intensity. The *q*-value is the corrected *P*-value, ranging from 0 to 1; a lower *q*-value indicates greater intensity. This figure shows the degree of enrichment for the top 20 pathways.

3.8. Validation of the identified DEGs through RT-qPCR

To confirm the accuracy of the 454 GS FLX sequencing results, the *CNGCs* (Fig. 7), *AUX1* (Fig. 8), *AHP* (Fig. 8), and *ATFBA7* (Fig. 9) randomly selected from above the three pathways were validated by the RT-qPCR. The differential expression levels of these genes observed by RT-qPCR were consistent with the results of 454 GS FLX sequencing (Fig. 10).

3.9. *ENO2* regulated the expression of *PGK*, *PGK1*, *TPI*, and *PK* was involved in the glycolytic pathway

To determine whether ENO2 interacts with PGK, PGK1, TPI, PK, and GAPC1, we performed yeast two-hybrid experiment. The resulting prey and bait vectors were co-transformed into the yeast strain AH109. The yeast transformants were isolated and assessed for growth on SD/-Trp-Leu (DDO) and SD/-Trp-Leu-His-Ade (QDO) medium. The results demonstrated that ENO2 interacted with PGK, PGK1, TPI, and PK (Fig. 11-A). The expression of *PGK* and *PGK1* genes, as indicated by the RT-qPCR, had an apparent reduction in the *eno2*$^{-}$ plants, but the expression of *TPI* and *PK* genes was not significantly different between the WT and *eno2*$^{-}$ plants under regular growth condition. The expression of *PGK*, *PGK1*, *TPI*, and *PK* genes were affected obviously in the *eno2*$^{-}$ plants after salt treatment (Fig. 11-B–E).

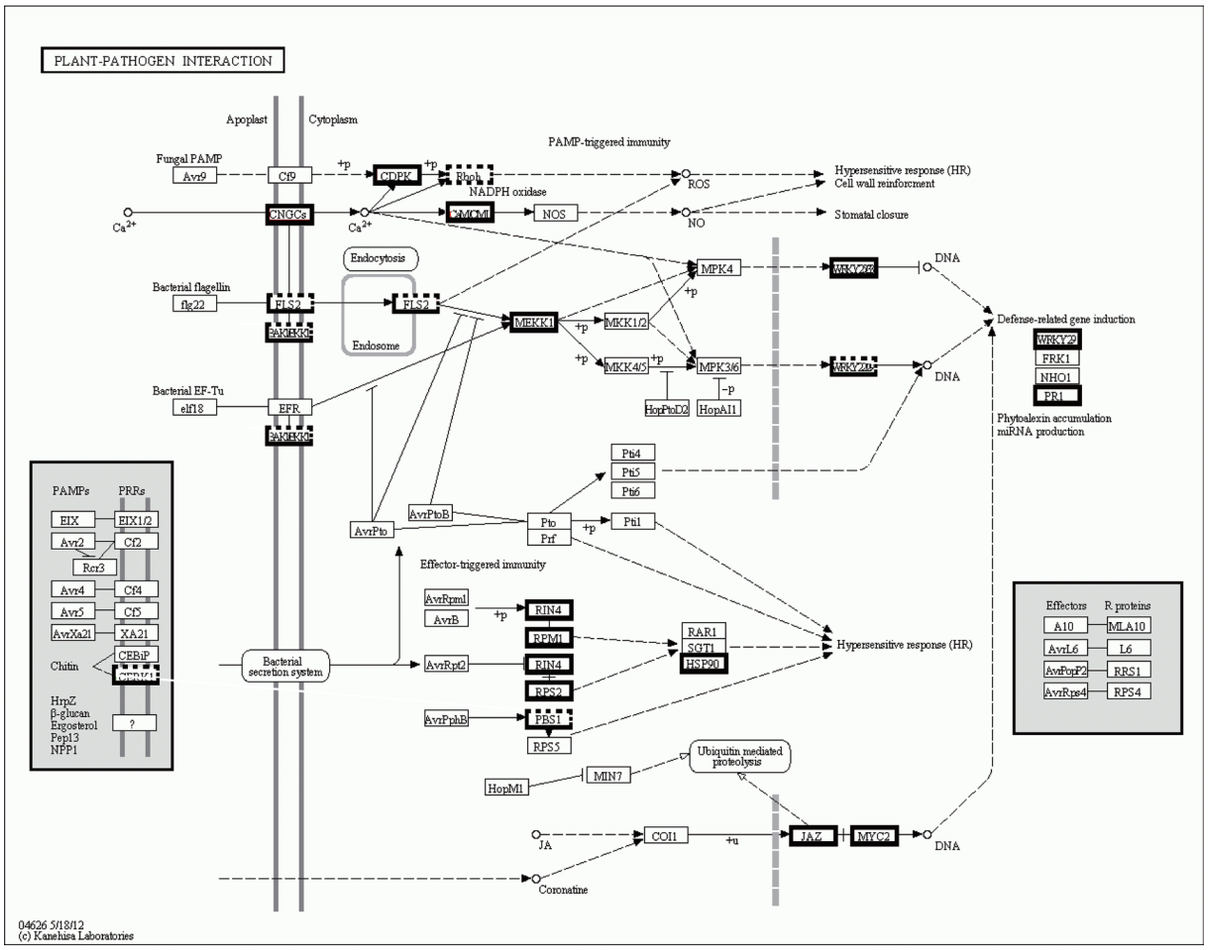

Fig. 7 Key enzymes and proteins regulating plant-pathogen interaction pathway. The genes encircled by bold solid line were up-regulated. The genes encircled by bold dashed line were down-regulation. Other genes are no change in expression.

4. Discussion

Salinity threatens approximately 20% of arable soil and 50% of irrigated land worldwide (Caruso *et al*. 2008). Salt stress is caused by excessive concentrations of salt, mainly in the form of NaCl, in the soil. In this study, *eno2*$^{-}$ mutant plants exposed to a high salt concentration displayed several prominent phenotypes (Fig. 1), which indicates that *AtENO2* is active in signal transduction pathways that are triggered by NaCl stress. Although research underlying the mechanism of *ENO2* tolerance in plant species has largely progressed in recent studies (Kang *et al*. 2013), it is still unclear how *ENO2* has led to the evolution of pathways that enables plants to withstand stress challenges in many biological environments. In the present study, the RT-qPCR and Western blotting results (Fig. 2) showed that *AtENO2* responded rapidly to 300 mmol L^{-1} NaCl stress. Namely, *AtENO2* played a more important role than *AtENO1* or *AtENO3*. *AtENO2* also played a greater role at high NaCl concentrations compared to other abiotic stresses, such as the cold, heat, and drought stress. The 454 GS FLX sequencing was used to investigate the causes of the different phenotypes and the multiple processes that were affected in the WT and *eno2*$^{-}$ *Arabidopsis* plants. Pathways, such as biosynthesis of secondary metabolites, plant-pathogen interactions (Fig. 7), and plant hormone signal transduction (Fig. 8), were highly influenced by high salinity. We also analyzed key enzymes and proteins that regulate glycolysis because ENO2 catalyzes a key step in glycolysis (Fig. 9). Based on our GO analysis, we realize that *ENO2* play a role in metabolic processes, response to stimuli; particularly the cellular processes, cellular development, membrane binding, and catalytic activity, among others. Previous studies have shown that cell wall components and cytoskeleton organization maintained cell turgor by transforming the cell size (Ndimba *et al*. 2005; Li *et al*. 2011). ENO2-GFP localizes in the nucleus as well as in the cytoplasm (Lee *et al*. 2002). The ENO2 promoter region

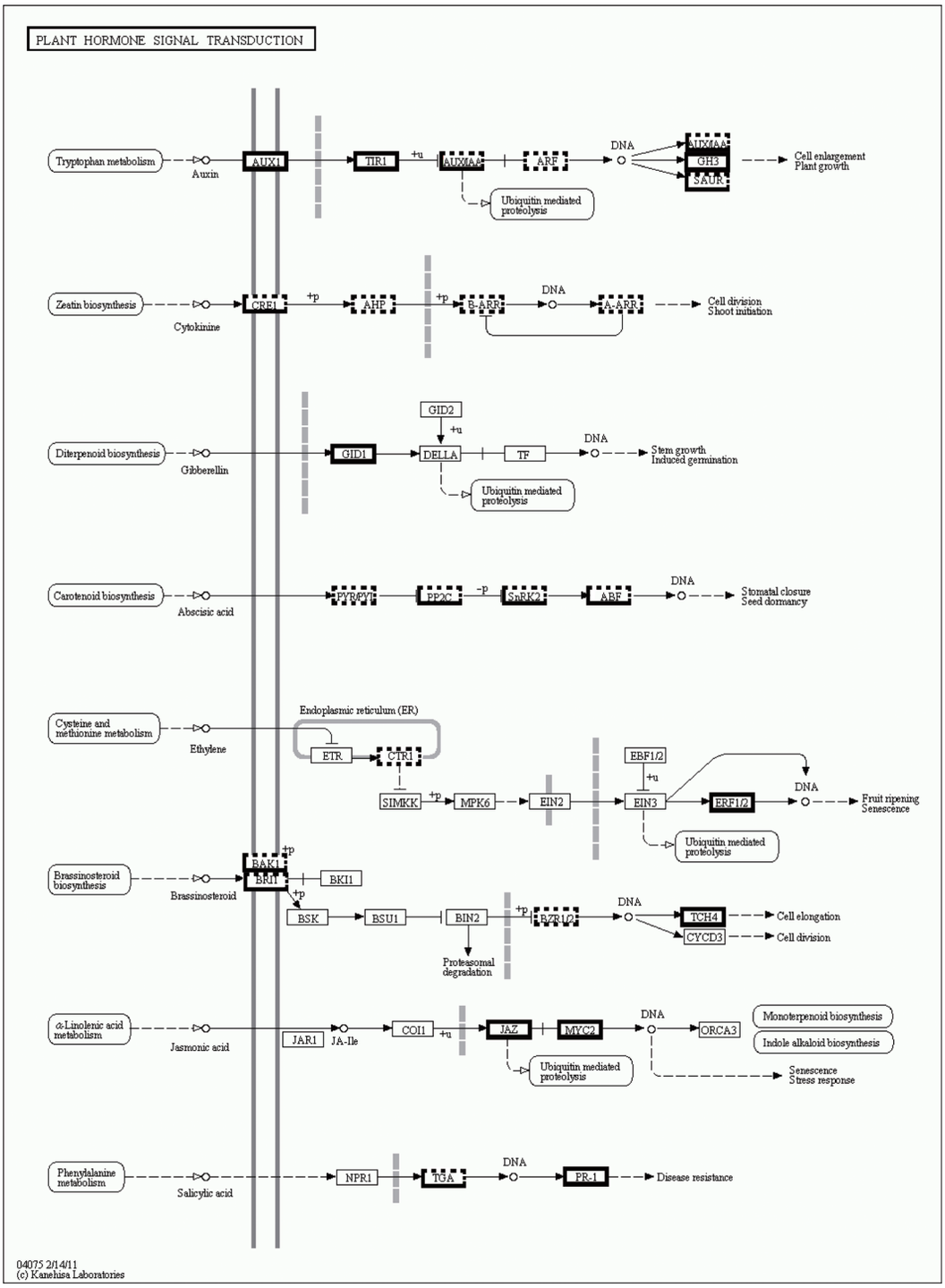

Fig. 8 Key enzymes and proteins regulating the plant hormone signal transduction pathway. The genes encircled by bold solid line were up-regulated. The genes encircled by bold dashed line were down-regulation and the genes encircled conjointly by bold solid and other genes are no change in expression.

was fused to the α-glucuronidase reporter gene (*GUS*), *GUS* expression was detected in all plant tissues (Lee *et al*. 2002). Analysis of fluorescence using confocal microscopy indicated that AtENO2-YFP was localized in both cytosolic and nuclear cellular compartments, while AtMBP-1-YFP was preferentially localized in nuclei (Kang *et al*. 2013; Eremina *et al*. 2015). DEGs with pathway annotations contributed to 115 pathways in the KEGG mapping analyses. The expression levels of the four genes validated using RT-qPCR confirmed the accuracy of the 454 sequencing

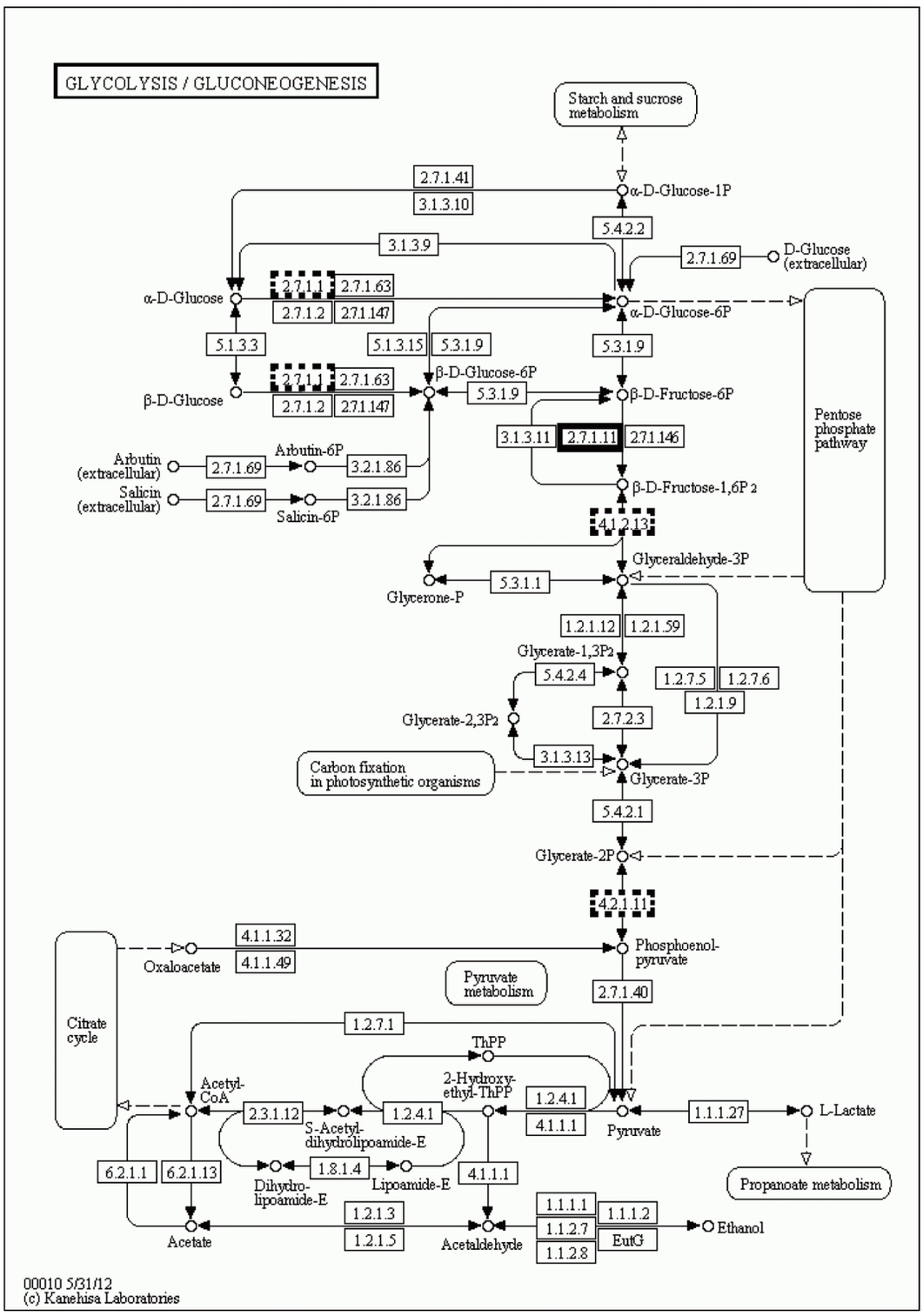

Fig. 9 Key enzymes and proteins regulating glycolysis. The number in the square represents the ID of the enzyme. The genes encircled by bold solid line were up-regulated. The genes encircled by bold dashed line were down-regulation. Other genes are no change in expression.

results (Fig. 10).

Because multi-genes regulate stress response, it is difficult to significantly enhance plant stress tolerance using a single functional gene approach (Mittler and Blumwald 2010). A large array of stress regulatory genes, such as TFs and protein kinases, have been authenticated in many

plants (Shinozaki *et al*. 2003). Progressively more studies have found that some TFs or protein kinases have vital roles in multiple abiotic stress tolerances (Banerjee and Roychoudhury 2015). The calcium-dependent protein kinase (CDPK) (Schaller *et al*. 2008) pathways and mitogen-activated protein kinase (MAPK) (Huang *et al*. 2012) involved in some plant stress responses. Three genes encoding the CDPK among the DEGs, namely, AT5G66210.4, AT4G04700.1 and AT4G04695.1, were up-regulated. In addition, another three genes encoding the MAPK among the DEGs, namely, AT1G01560.1, AT1G01560.2 and AT5G67080.1 were also up-regulated. This shows that *ENO2* is very important in stress responses.

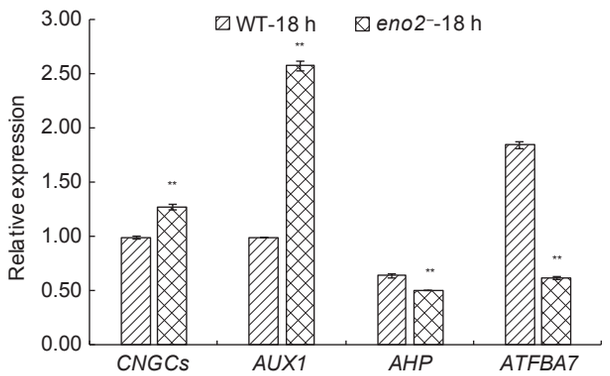

Fig. 10 The relative expression levels of *CNGCs*, *AUX1*, *AHP*, and *ATFBA7*. *CNGCs*, *AUX1*, *AHP*, and *ATFBA7* were randomly selected from differentially expressed genes (DEGs) in response to 300 mmol L^{-1} NaCl stress, as revealed by quantitative real-time RT-PCR (RT-qPCR) analysis. 30-d-old wild type (WT) and *ENO2* T-DNA insertion mutant (*eno2*$^{-}$) plants were treated with 300 mmol L^{-1} NaCl for 18 h. * and **, significances at $P<0.05$ and $P<0.01$, respectively. Bars represent the values of stand error.

Many abiotic stresses can weaken plant defense mechanisms (Amtmann *et al*. 2008; Mittler and Blumwald 2010; Atkinson and Urwin 2012). Because NaCl is known as an antifungal agent (Blomberg and Adler 1993), salt stress-pathogen interactions may be highly affected by stress concentrations (Souman and Kostandi 1998; Poschenrieder *et al*. 2006; Fones *et al*. 2010). Our results (Fig. 7) were consistent with previous researches.

Additionally, hormones play a role in the integration of environmental stimuli under stress conditions (Kissoudis *et al*. 2014). The growth hormones, gibberellin, cytokinin, auxin, and brassinosteroid are active in response to adverse situations and pathogen attack (Robert-Seilaniantz *et al*. 2011). Abscisic acid produced under high salinity conditions regulates stomatal closure and activates many stress-related genes to increase tolerance of plant to stresses (Nakashima

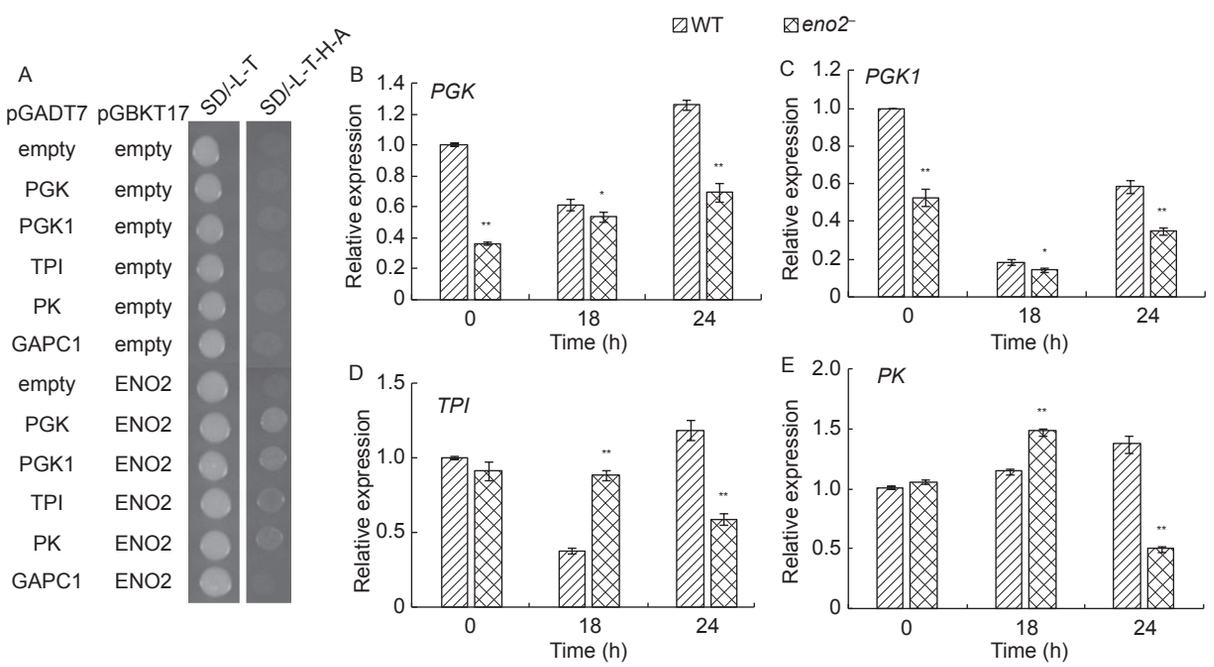

Fig. 11 Interactions of *ENO2* with *PGK*, *PGK1*, *TPI*, and *PK* under salt stress. A, yeast cells were co-transformed with the PGK, PGK1, TPI, and PK, pGBKT7-ENO2 (bait) constructs and the pGADT7 empty vector, pGBKT7-ENO2 proteins (bait) and all four pGADT7-PGK, pGADT7-PGK1, pGADT7-TPI, and pGADT7-PK proteins (prey) were grown on yeast SD drop-out medium that lacks Leu and Trp (-2) and Ade, His, Leu, and Trp (-4). B–E, the relative expression levels of *PGK*, *PGK1*, *TPI*, and *PK* in the wild type (WT) and *ENO2* T-DNA insertion mutant (*eno2*$^{-}$) plants. * and **, significances at $P<0.05$ and $P<0.01$, respectively. Bars represent the values of stand error.

et al. 2012). Ethylene participates in BR-induced AOX activity, which is important in the tolerance to abiotic stresses (Wei *et al*. 2015). Jasmonic acid (JA) is ubiquitous in plants (Schaller 2011; Pirbalouti *et al*. 2014). Under certain abiotic stresses, in particular salt stress, the application of exogenous JA was effective to improve tolerance of plants to stresses (Ahmad *et al*. 2016). Salicylic acid (SA) is a phenolic compound that triggers hypersensitive response to defense biotrophic pathogens (Eremina *et al*. 2016). It has also been reported that SA induces salinity tolerance by eventually activating the photosynthetic process and alleviating oxidative stress (Li *et al*. 2014). Thus, our study further confirms and supplements previous research investigating the relationship between abiotic stress and plant hormones.

Interestingly, only one protein family in the glycolysis pathway was up-regulated. This finding suggests that the molecular responses of *ENO2* to abiotic stresses involve interactions among many pathways in addition to the glycolysis pathway. Therefore, it is very difficult to increase salt tolerance in complex organisms such as plants using only one approach.

PGK is an ATP-generating enzyme, a part of the glycolytic, photosynthetic, and gluconeogenic pathways (Banks *et al*. 1979; McHarg *et al*. 1999; Lin *et al*. 2007). Ectopic expression of Pokkali phosphoglycerate kinase-2 (OsPGK2-P) improved yield in tobacco (*Nicotiana tabaccum* L.) plants under salinity stress (Joshi *et al*. 2016). *TPI* involved in response to a variety of abiotic stress in rice (*Oryza sativa* L.) (Sharma *et al*. 2012). *PK* was induced in soybean under flooding conditions and induced metabolic changes that promoted survival and recovery from flooding-induced damage (Khan *et al*. 2015). Results from the yeast two-hybrid assay showed that ENO2 interacts with other glycolysis enzymes such as PGK, PGK1, TPI, and PK (Fig. 11-A). Most importantly, the expression of *PGK* and *PGK1* had an apparent reduction in the *eno2*$^{-}$ plants (Fig. 11-B–C), and *ENO2* may regulate the expression of *PGK*, *PGK1*, *TPI*, and *PK* under salt stress (Fig. 11-B–E). The exceptions of these differences from the sequencing data in expression may result from the different criteria. For RT-qPCR analysis, it is relative expression level, but for sequencing, it is RPKM (reads per kiobase million reads). This result suggested that *ENO2* had an important role in the plant growth and response to the high salt stress in some ways.

5. Conclusion

In summary, we sequenced the WT and *eno2*$^{-}$ mutant *Arabidopsis* lines that were stressed with 300 mmol L^{-1} NaCl for 18 h using the 454 GS FLX platform and identified a large number of DEGs. Our EST database can serve as a valuable resource for genetic and genomic studies of *Arabidopsis* mutants in response to salt stress. The present findings highlight the diverse modes of adaptation to salt stress, and additional research such as proteomics studies and determination of enzyme activities will be essential to elucidate the related regulatory mechanisms.

Acknowledgements

This study was funded by the National Natural Science Foundation of China (31470399 and 31270365). We thank BGI-Tech Solutions Co., Ltd. (BGI-Tech, China) for performing the transcriptome sequencing.

Appendix associated with this paper can be available on http://www.ChinaAgriSci.com/V2/En/appendix.htm

References

Ahmad P, Prasad M N. 2012. *Abiotic Stress Responses in Plants*: *Metabolism, Productivity and Sustainability*. Springer-Verlag, New York.

Ahmad P, Rasool S, Gul A, Sheikh S A, Akram N A, Ashraf M, Kazi A M, Gucel S. 2016. Jasmonates: Multifunctional roles in stress tolerance. *Frontiers in Plant Science*, **7**, 813.

Altschul S F. 1993. A protein alignment scoring system sensitive at all evolutionary distances. *Journal of Molecular Evolution*, **3**, 290–300.

Amtmann A, Troufflard S, Armengaud P. 2008. The effect of potassium nutrition on pest and disease resistance in plants. *Plant Physiology*, **4**, 682–691.

Andriotis V M, Kruger N J, Pike M J, Smith A M. 2010. Plastidial glycolysis in developing *Arabidopsis* embryos. *New Phytologist*, **3**, 649–662.

Atkinson N J, Urwin P E. 2012. The interaction of plant biotic and abiotic stresses: From genes to the field. *Journal of Experimental Botany*, **10**, 3523–3543.

Banerjee A, Roychoudhury A. 2015. WRKY proteins: Signaling and regulation of expression during abiotic stress responses. *Scientific World Journal*, **2015**, 807560.

Banks R D, Blake C C, Evans P R, Haser R, Rice D W, Hardy G W, Merrett M, Phillips A W. 1979. Sequence, structure and activity of phosphoglycerate kinase: A possible hinge-bending enzyme. *Nature*, **279**, 773–777.

Barkla B J, Vera-Estrella R, Hernández-Coronado M, Pantoja O. 2009. Quantitative proteomics of the tonoplast reveals a role for glycolytic enzymes in salt tolerance. *The Plant Cell*, **12**, 4044–4058.

Bent A F, Mackey D. 2007. Elicitors, effectors, and R genes: The new paradigm and a lifetime supply of questions. *Annual Review of Phytopathology*, **45**, 399–436.

Blakeley S D, Dekroon C, Cole K P, Kraml M, Dennis D T. 1994. Isolation of a full-length cDNA encoding cytosolic enolase from *Ricinus communis*. *Plant Physiology*, **1**, 455–456.

Blomberg A, Adler L. 1993. Tolerance of fungi to NaCl. In: Jennings D H, ed., *Stress Tolerance of Fungi*. Marcel Dekker, New York. pp. 209–232.

Bray A. 1997. Plant responses to water deficit. *Trends in Plant Science*, **2**, 48–54.

Bray E A, Bailey-Serres J, Weretilnyk E. 2000. Responses to abiotic stresses. In: Gruissem W, Buchnnan B, Jones R, eds., *Biochemistry and Molecular Biology of Plants*. American Society of Plant Physiologists, Rockville, MD. pp. 1158–1249.

Caruso G, Cavaliere C, Guarino C, Gubbiotti R, Foglia P, Laganà A. 2008. Identification of changes in *Triticum durum* L. leaf proteome in response to salt stress by two-dimensional electrophoresis and MALDI-TOF mass spectrometry. *Analytical and Bioanalytical Chemistry*, **1**, 381–390.

Conesa A, Götz S, García-Gómez J M, Terol J, Talón M, Robles M. 2005. Blast2GO: A universal tool for annotation, visualization and analysis in functional genomics research. *Bioinformatics*, **18**, 3674–3676.

Eremina M, Rozhon W, Poppenberger B. 2016. Hormonal control of cold stress responses in plants. *Cellular and Molecular Life Sciences*, **4**, 797–810.

Eremina M, Rozhon W, Yang S, Poppenberger B. 2015. ENO2 activity is required for the development and reproductive success of plants, and is feedback-repressed by AtMBP-1. *The Plant Journal*, **6**, 895–906.

Fones H, Davis C A, Rico A, Fang F, Smith J A, Preston G M. 2010. Metal hyperaccumulation armors plants against disease. *PLoS Pathogens*, **9**, e1001093.

Holland M J, Holland J P. 1978. Isolation and identification of yeast messenger ribonucleic acids coding for enolase, glyceraldehyde-3-phosphate dehydrogenase, and phosphoglycerate kinase. *Biochemistry*, **23**, 4900–4907.

Huang G T, Ma S L, Bai L P, Zhang L, Ma H, Jia P, Liu J, Zhong M, Guo Z F. 2012. Signal transduction during cold, salt, and drought stresses in plants. *Molecular Biology Reports*, **2**, 969–987.

Jiang Y, Yang B, Harris N S, Deyholos M K. 2007. Comparative proteomic analysis of NaCl stress-responsive proteins in *Arabidopsis* roots. *Journal of Experimental Botany*, **13**, 3591–3607.

Joshi R, Karan R, Singla-Pareek S L, Pareek A. 2016. Ectopic expression of Pokkali phosphoglycerate kinase-2 (OsPGK2-P) improves yield in tobacco plants under salinity stress. *Plant Cell Reports*, **1**, 27–41.

Kang M, Abdelmageed H, Lee S, Reichert A, Mysore K S, Allen R D. 2013. AtMBP-1, an alternative translation product of LOS2, affects abscisic acid responses and is modulated by the E3 ubiquitin ligase AtSAP5. *The Plant Journal*, **3**, 481–493.

Khan M N, Sakata K, Komatsu S. 2015. Proteomic analysis of soybean hypocotyl during recovery after flooding stress. *Journal of Proteomics*, **121**, 15–27.

Kissoudis C, van de Wiel C, Visser R G, van der Linden G. 2014. Enhancing crop resilience to combined abiotic and biotic stress through the dissection of physiological and molecular crosstalk. *Frontiers in Plant Science*, **5**, 207.

Lal S K, Johnson S, Conway T, Kelley P M. 1991. Characterization of a maize cDNA that complements an enolase-deficient mutant of *Escherichia coli*. *Plant Molecular Biology*, **5**, 787–795.

Lee H, Guo Y, Ohta M, Xiong L, Stevenson B, Zhu K. 2002. LOS2, a genetic locus required for cold-responsive gene transcription encodes a bi-functional ENOLASE. *EMBO Journal*, **11**, 2692–2702.

Li T, Hu Y, Du X, Tang H, Shen C, Wu J. 2014. Salicylic acid alleviates the adverse effects of salt stress in *Torreya grandis cv*. Merrillii seedlings by activating photosynthesis and enhancing antioxidant systems. *PLOS ONE*, **10**, e109492.

Li W, Zhang C, Lu Q, Wen X, Lu C. 2011. The combined effect of salt stress and heat shock on proteome profiling in *Suaeda salsa*. *Journal of Plant Physiology*, **15**, 1743–1752.

Lin J W, Ding M P, Hsu Y H, Tsai C H. 2007. Chloroplast phosphoglycerate kinase, a gluconeogenetic enzyme, is required for efficient accumulation of *Bamboo mosaic virus*. *Nucleic Acids Research*, **35**, 424–432.

Liu X, Zhang H, Zhao Y, Feng Z, Li Q, Yang HQ, Luan S, Li J, He Z H. 2013. Auxin controls seed dormancy through stimulation of abscisic acid signaling by inducing ARF-mediated ABI3 activation in *Arabidopsis*. *Proceedings of the National Academy of Sciences of the United States of America*, **38**, 15485–15490.

McHarg J, Kelly S M, Price N C, Cooper A, Littlechild J A. 1999. Site-directed mutagenesis of proline 204 in the 'hinge' region of yeast phosphoglycerate kinase. *European Journal of Biochemistry*, **259**, 939–945.

Mickelbart M V, Hasegawa P M, Bailey-Serres J. 2015. Genetic mechanisms of abiotic stress tolerance that translate to crop yield stability. *Nature Reviews Genetics*, **4**, 237–251.

Mittler R. 2006. Abiotic stress, the field environment and stress combination. *Trends in Plant Science*, **1**, 15–19.

Mittler R, Blumwald E. 2010. Genetic engineering for modern agriculture: Challenges and perspectives. *Annual Review of Plant Biology*, **61**, 443–462.

Nakashima K, Takasaki H, Mizoi J, Shinozaki K, Yamaguchi-Shinozaki K. 2012. NAC transcription factors in plant abiotic stress responses. *Biochimica et Biophysica Acta*, **2**, 97–103.

Ndimba B K, Chivasa S, Simon W J, Slabas A R. 2005. Identification of *Arabidopsis* salt and osmotic stress responsive proteins using two-dimensional difference gel electrophoresis and mass spectrometry. *Proteomics*, **16**, 4185–4196.

Pieterse C M, van der Does D, Zamioudis C, Leon-Reyes A, van Wees S C. 2012. Hormonal modulation of plant immunity. *Annual Review of Cell and Developmental Biology*, **28**, 489–521.

Pirbalouti A G, Mirbagheri H, Hamedi B, Rahimi E. 2014. Antibacterial activity of the essential oils of myrtle leaves against *Erysipelothrix rhusiopathiae*. *Asian Pacific Journal of Tropical Biomedicine*, **4**, 505–509.

Poschenrieder C, Tolrà R, Barceló J. 2006. Can metals defend plants against biotic stress? *Trends in Plant Science*, **6**, 288–295.

Rangan P, Subramani R, Kumar R, Singh A K, Singh R. 2014. Recent advances in polyamine metabolism and abiotic stress tolerance. *Biomed Research International*, **2014**, 239621.

Reed G H, Poyner R R, Larsen T M, Wedekind J E, Rayment I. 1996. Structural and mechanistic studies of enolase. *Current Opinion in Structural Biology*, **6**, 736–743.

Robert-Seilaniantz A, Grant M, Jones J D. 2011. Hormone crosstalk in plant disease and defense: More than just JASMONATE-SALICYLATE antagonism. *Annual Review of Phytopathology*, **49**, 317–343.

Rothberg J M, Leamon J H. 2008. The development and impact of 454 sequencing. *Nature Biotechnology*, **26**, 1117–1124.

Sachs M M, Freeling M, Okimoto R. 1980. The anaerobic proteins of maize. *Cell*, **3**, 761–767.

Schaller G E, Kieber J J, Shiu S H. 2008. Two-component signaling elements and histidyl-aspartyl phosphorelays. *Arabidopsis Book*, **6**, e0112.

Schaller M. 2011. The behavioral immune system and the psychology of human sociality. *Philosophical Transactions of the Royal Society of London Series B* (Biological Sciences), **1583**, 3418–3426.

Sharma S, Mustafiz A, Singla-Pareek S L, Srivastava P S, Sopory S K. 2012. Characterization of stress and methylglyoxal inducible triose phosphate isomerase (OscTPI) from rice. *Plant Signaling & Behavior*, **10**, 1337–1345.

Shao H, Wang H, Tang X. 2015. NAC transcription factors in plant multiple abiotic stress responses: Progress and prospects. *Frontiers in Plant Science*, **6**, 902.

Shi H, Ye T, Chen F, Cheng Z, Wang Y, Yang P, Zhang Y, Chan Z. 2013. Manipulation of arginase expression modulates abiotic stress tolerance in *Arabidopsis*: Effect on arginine metabolism and ROS accumulation. *Journal of Experimental Botany*, **5**, 1367–1379.

Shinozaki K, Yamaguchi-Shinozaki K, Seki M. 2003. Regulatory network of gene expression in the drought and cold stress responses. *Current Opinion in Plant Biology*, **5**, 410–417.

Souman M F, Kostandi S F. 1998. Effect of saline environment on yield and smut disease severity of different corn genotypes (*Zea mays* L.). *Journal of Phytopathology*, **4**, 185–189.

van der Straeten D, Rodrigues-Pousada R A, Goodman H M, van Montagu M. 1991. Plant enolase: Gene structure, expression and evolution. *The Plant Cell*, **7**, 719–735.

Umeda M, Uchimiya H. 1994. Differential transcript levels of genes associated with glycolysis and alcohol fermentation in rice plants (*Oryza sativa* L.) under submergence stress. *Plant Physiology*, **3**, 1015–1022.

Voll L M, Hajirezaei M R, Czogalla-Peter C, Lein W, Stitt M, Sonnewald U, Börnke F. 2009. Antisense inhibition of enolase strongly limits the metabolism of aromatic amino acids, but has only minor effects on respiration in leaves of transgenic tobacco plants. *New Phytologist*, **3**, 607–618.

Wang H, Wang H, Shao H, Tang X. 2016. Recent advances in utilizing transcription factors to improve plant abiotic stress tolerance by transgenic technology. *Frontiers in Plant Science*, **7**, 67.

Wei L J, Deng X G, Zhu T, Zheng T, Li P X, Wu J Q, Zhang D W, Lin H H. 2015. Ethylene is involved in Brassinosteroids induced alternative respiratory pathway in cucumber (*Cucumis sativus* L.) seedlings response to abiotic stress. *Frontiers in Plant Science*, **6**, 982.

Yan S P, Tang Z, Su W, Sun W. 2005. Proteomic analysis of salt stress-responsive proteins in rice root. *Proteomics*, **1**, 235–244.

Section editor ZHANG Xue-yong
Managing editor WANG Ning